

Near-Field Focused Folded Transmitarray Antenna for Medical Applications

Saber H. Zainud-Deen^{1*}, Walaa M. Hassan², and Hend A. Malhat^{1**}

¹ Department of Electronics and Communication Engineering
Faculty of Electronic Eng., Menoufia, Egypt
*anssaber@yahoo.com, **er_honidal@yahoo.com

² Department of Microwave Engineering
Electronics Research Institute, Giza, 12622, Egypt
walaa81hassan@yahoo.com

Abstract — A near-field focused folded transmitarray antenna is proposed at 2.45 GHz for medical applications. The proposed folded transmitarray construction introduces compact design, low profile, and reduced fabrication cost with focused power in both the near-field and far-field regions of the antenna. The transmitarray consists of a feeding horn antenna embedded centrally in the transmitarray structure and a perfect electric conductor plate with the same size as a reflector. The radiation from the feeding horn is reflected by the plate toward the transmitarray. The unit-cell element of the transmitarray is a square dielectric box with four identical circular holes. The transmission coefficient was nearly -3 dB in magnitude and 320 degrees in phase. The radiation characteristics of the unfolded and folded transmitarray are analyzed using the finite integral technique. The normalized power density distribution around a part of the human leg placed in front of the transmitarray is investigated. The proposed antenna is used to heat a specific area on the human leg for treatment.

Index Terms — Folded, medical applications, near-field focused, transmitarray.

I. INTRODUCTION

Large aperture antennas are attractive to space applications such as satellite communications, radar systems, and radio astronomy. The most requirements of these applications are the compact structure, high-gain, low production cost and low loss. High gain can be obtained using different antennas, like parabolic reflector, phased array, reflectarray, and transmitarray [1-4]. The disadvantages of the parabolic reflectors are generally being bulky in size, heavy, and large supporting structures. Phased array suffers from network feeding losses and complexity. Reflectarray and transmitarray are easy to fabricate, low profile and have no insertion loss. Reflectarray antenna combines the features of the parabolic reflector and the phased array. It is a planer

surface with discrete elements which transform the spherical wave to the plane wave by adding a compensation phase shift. Although the reflectarray has light weight and it is simple to fabricate, it still requires an offset feed to avoid blockage losses. The offset geometry destroys the symmetry of an antenna aperture and increases the angle of incident wave, thus reducing the reflector's gain, decreasing efficiency and complicating the design. In the transmitarray, there is no need for offset feed design. The transmitarray combines the features of lens and phased array antenna. Transmitarray has the same structure of the reflectarray but with opposite beam direction. Transmitarray overcomes the blockage losses in the reflectarray. In open literature, the transmission coefficient magnitude extended from 0 to -4 dB and phase variation of 300 degrees are enough to design the transmitarray [5,6]. Folded transmitarray antennas are compact shape of the transmitarrays. Although transmitarrays employ planar printed structures, they typically require a reasonable depth according to the focal distance of the feed. A reduction of the antenna depth by a factor of about two is achieved using a folded reflectarray as demonstrated in [7-10].

Near-field (NF) focused antennas have been studied over a long time [11-12]. The general purpose of using focused antennas is to concentrate the electromagnetic power in a certain relatively small region of space usually is called the focus (spot). NF-focused antennas have different applications such as microwave remote sensing, local hyperthermia, thermography, and imaging [13-14]. NF-focused microstrip arrays have been designed for gate-access control and management [15]. Radio-frequency identification (RFID) has been introduced as a proper application for NF-focused antennas [16-21]. More recently, NF-focused array microstrip planar antenna for medical applications is investigated in [22]. The NF-focused antennas are needed to concentrate power in a desired spot area to heat a certain tissue without heating adjacent tissues [13, 14]. They depend

on phase control of the radiation sources on the antenna's aperture in such a way that all their contributions sum in phase at a specific focal point, located in the antenna's near field region. NF-focused antennas can be realized by pyramidal or conical horns, by resorting to a lens in front of the antenna aperture. Alternative solutions are based on either reflector antennas or Fresnel-zone antennas [11]. Another method for NF-focused antenna [13-14] is used of the planar microstrip arrays, with a feeding network, which suffers from complicated beam forming networks, complex feeding circuit and relatively high power loss.

In the present paper, a NF-focused folded transmitarray working on 2.45 GHz for medical application is proposed. The antenna consists of a feeding horn antenna embedded centrally in transmitarray structure and a perfect electric conducting (PEC) plate with the same size of the transmitarray as a reflector. The optimization of the plate position relative to the transmitarray aperture has been investigated. In the proposed antenna, the antenna depth is reduced by a factor of two compared to that required for the un-folded transmitarray. The transmitarray is made from one piece of dielectric material sheet, with a perforated dielectric and completely eliminating all the rest of the dielectric materials. The simplicity of the structure makes it practical in terms of cost, space, and ease to fabricate. Finally, the effect of the NF-focused folded transmitarray on the human leg has been investigated. All the radiation characteristics of the transmitarrays has been analyzed using the CST-microwave studio [25].

II. DESIGN OF THE UNIT-CELL

The configuration of the proposed transmitarray unit-cell element is shown in Fig. 1. It consists of a square dielectric box, with arm length $L = 60$ mm, thickness $h = 60$ mm, and dielectric constant $\epsilon_r = 12$. Each unit-cell element has four identical circular holes. Each hole has radius r . The required transmission coefficient phase and magnitude compensations of each unit-cell element are achieved by varying the hole radius using the waveguide simulator. The perfect electric and magnetic wall boundary conditions are applied to the sides of the surrounding waveguide, and result in image planes on all sides of the unit-cell element to represent an infinite array approximation. A normal incident plane wave was used as the excitation of the unit-cell element inside the waveguide simulator. The variations of the transmission coefficient, phase and magnitude, versus hole radius at 2.45 GHz are shown in Fig. 2. The transmission coefficient phase variation is changed from 0 to 320 degrees, while the transmission coefficient magnitude is varied from 0 to -3.2 dB. The hole radius is changed from 5 to 15 mm. The results are calculated using the CST MWS and compared with that calculated using the HFSS software. Good agreement is achieved.

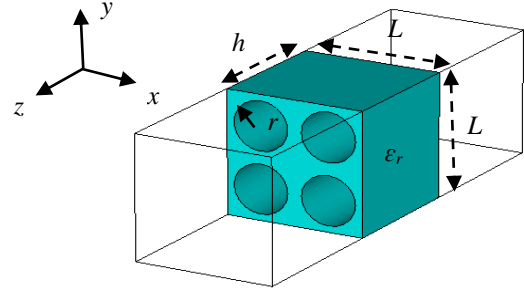


Fig. 1. Transmitarray unit-cell element design at 2.45 GHz.

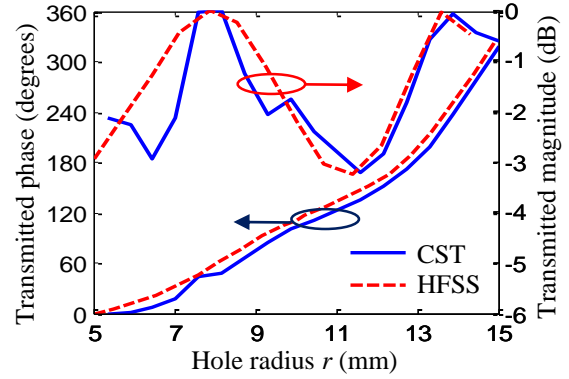


Fig. 2. The variations of the transmission coefficient, phase and magnitude, versus the hole radius at 2.45 GHz.

III. DESIGN OF THE TRANSMITARRAY AND FOLDED TRANSMITARRAY

Figure 3 (a) shows 9×9 transmitarray placed in x - y plane with total area of 54×54 cm². A linearly polarized horn antenna is used to feed transmitarray with dimensions $R_i = 10.2$ cm, $l_i \times w_i = 4.65 \times 9.3$ cm² and thickness $t = 0.5$ cm. Horn antenna is located at a distance F normal to the transmitarray aperture. The required phase compensation ϕ_{ij} at each unit-cell element in the transmitarray to collimate a beam in the (θ_o, ϕ_o) direction is obtained by:

$$\phi_{ij}(x_{ij}, y_{ij}) = k_o [d_{ij} - x_{ij} \sin(\theta_o) \cos(\phi_o) - y_{ij} \sin(\theta_o) \sin(\phi_o)], \quad (1)$$

where $d_{ij} = \sqrt{(x_{ij} - x_f)^2 + (y_{ij} - y_f)^2 + z_f^2}$, (2)

k_o is the propagation constant, d_{ij} is the distance from the feed point (x_f, y_f, z_f) to the ij^{th} element in the array located at (x_{ij}, y_{ij}) . Table 1 lists the required compensation phases and the corresponding holes radii for the transmitarray. A compact folded transmitarray antenna is shown in Fig. 3 (b). It consists of a feeding horn antenna embedded centrally in the transmitarray structure and a PEC plate with the same size of the transmitarray acts as a reflector located at a distance $F/2$ normal to the transmitarray aperture. The radiation from the feeding horn is reflected back by the PEC plate toward the transmitarray. The E-plane and H-plane radiation patterns for unfolded

transmitarray, folded transmitarray and horn antenna at frequency 2.45 GHz are shown in Fig. 4. The unfolded transmitarray introduces maximum gain of 21.4 dBi with first side lobe level (SLL) of -16.4 dB / -17.9 dB in the E-plane /H-plane. The folded transmitarray introduces maximum gain of 21.4 dBi with SLL of -11.6 dB / -12.3 dB in the E-plane/H-plane. The variations of the gain versus frequency are shown in Fig. 5. The same maximum gain of the unfolded transmitarray and folded transmitarray at 2.45 GHz is achieved. The 1-dB gain bandwidth for the unfolded transmitarray is 1.7 GHz compared to 200 MHz for folded transmitarray. The NF-focusing of the transmitarray is achieved by appending an extra phase shift to the elements of the transmitarray to collimate the beam at a focal point R_o as shown in Fig. 6. The extra phase shift of the ij^{th} element can be calculated from [23]:

$$\phi_{ijNF} = \frac{2\pi}{\lambda} \left(\sqrt{x_{ij}^2 + y_{ij}^2 + R_o^2} - R_o \right). \quad (3)$$

The total phase for NF-focused folded transmitarray is obtained by adding the phase in Eq. (1) with the corresponding extra phase in Eq. (3). The focal plane is very close to the near edge of the Fresnel region, so it causes that the ratio of active power density to the reactive power density is very large. Table 2 lists the compensation phases and the corresponding holes radii for the first quadrant of the NF-focused transmitarray.

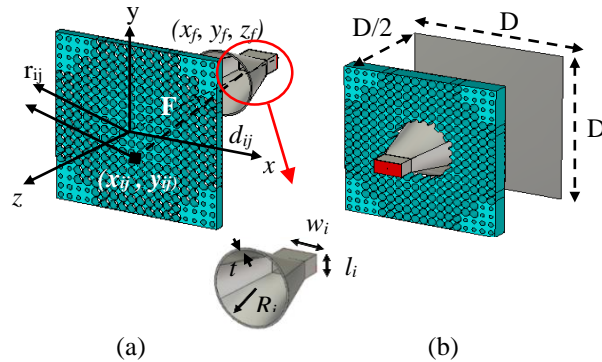
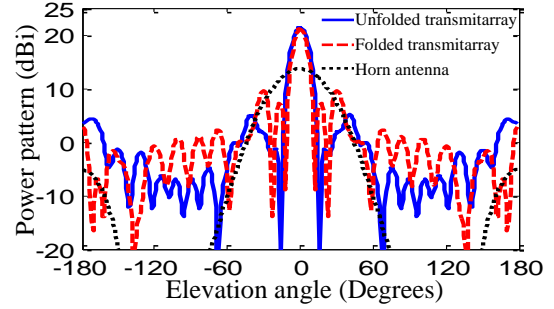


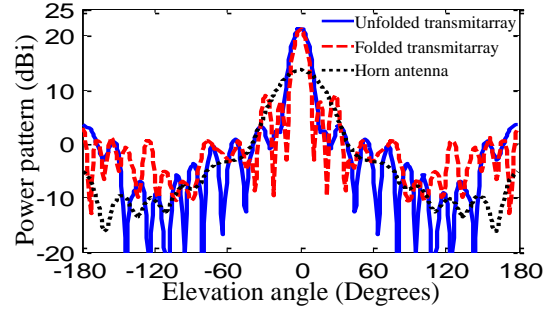
Fig. 3. (a) The 3-D detailed construction of 9×9 unfolded transmitarray, and (b) the 3-D detailed construction of 9×9 folded transmitarray.

Table 1: The compensation phases and the corresponding holes radii for the first quadrant of the transmitarray

147.6°	157.36°	186.32°	233.47°	297.33°
12 mm	12.33 mm	13.05 mm	13.81 mm	14.7 mm
157.36°	167.08°	195.86°	242.74°	306.27°
12.33 mm	12.62 mm	13.22 mm	13.94 mm	14.8 mm
186.32°	195.86°	224.15°	270.26°	332.79°
13.05 mm	13.22 mm	13.68 mm	14.32 mm	15 mm
233.47°	242.74°	270.26°	315.15°	16.14°
13.81 mm	13.94 mm	14.32 mm	14.96 mm	7 mm
297.33°	306.27°	332.79°	16.14°	75.15°
14.7 mm	14.83 mm	15 mm	7 mm	9 mm



(a) E-plane (x-z)



(b) H-plane (y-z)

Fig. 4. The E-plane and H-plane radiation patterns variations versus the elevation angle for configuration 9×9 unfolded transmitarray, folded transmitarray and the horn antenna for $F/D = 1$, and $f = 2.45$ GHz.

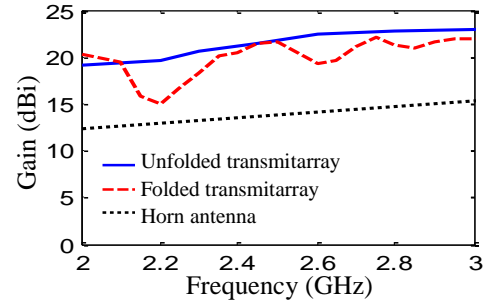


Fig. 5. The variations of the gain versus frequency for 9×9 unfolded transmitarray, folded transmitarray and the horn antenna for $F/D = 1$, and $f = 2.45$ GHz.

Table 2: The compensation phases and the corresponding holes radii for the first quadrant of the NF-focused transmitarray

147.6°	157.36°	186.32°	233.47°	297.33°
12 mm	12.54 mm	13.55 mm	14.71 mm	8.29 mm
157.36°	167.08°	195.86°	242.74°	306.27°
12.54 mm	12.95 mm	13.7 mm	14.96 mm	8.75 mm
186.32°	195.86°	224.15°	270.25°	332.79°
13.55 mm	13.79 mm	14.49 mm	6.12 mm	10.62 mm
233.47°	242.74°	270.26°	315.18°	16.14°
14.71 mm	14.96 mm	6.12 mm	9.26 mm	13.16 mm
297.33°	306.27°	332.79°	16.14°	75.15°
8.29 mm	8.75 mm	10.62 mm	13.16 mm	14.71 mm

The 3-dB beamwidth in the focal plane is defined as folded transmitarray spot area. The spot area radius W of the near field focused folded transmitarray is given by [24]:

$$W = 0.8868 R_o \cdot \frac{\lambda_o}{D}, \quad (4)$$

where D is the total transmitarray length. Contour plot of the normalized power density for the non-focused unfolded transmitarray, non-focused folded transmitarray, and NF-focused folded transmitarray on the array aperture in x - y plane at $R_o = 72$ cm (focal plane) are shown in Fig. 6. The contour lines are closer to each other for the NF-focused folded transmitarray compared to the other two cases. The radius of the 3-dB spot area for the NF-focused folded transmitarray is $W = 7.5$ cm at the focal plane while it is 12.3 cm for the non-focused unfolded transmitarray and 8 cm for non-focused folded transmitarray. Figure 7 shows the power density in dB versus the axial distance from the antenna aperture. The maximum occurs at a distance about 40 cm from the aperture of the transmitarray.

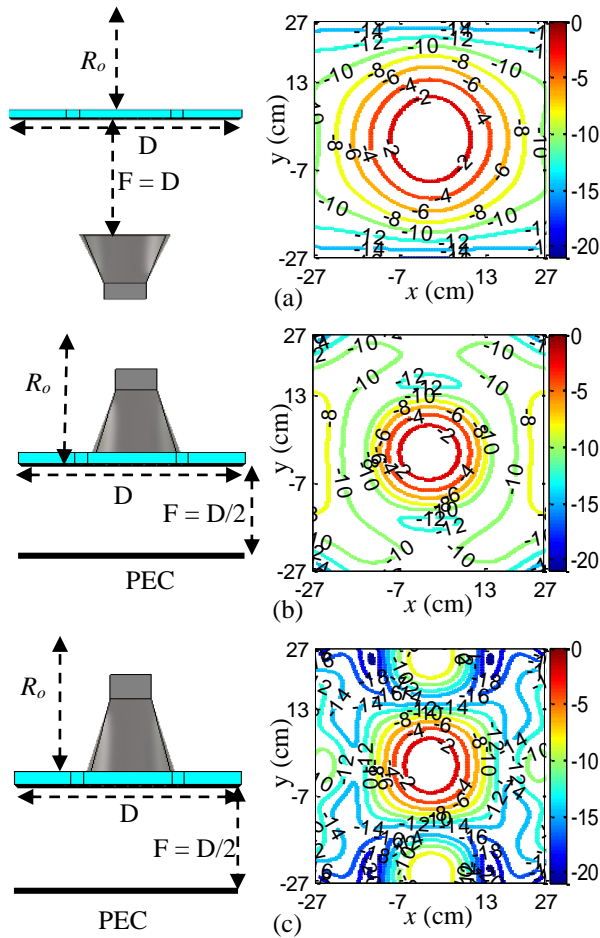


Fig. 6. A contour plot of the normalized power density at distance $R_o = 72$ cm (focal plane) for: (a) non-focused unfolded transmitarray, (b) non-focused folded transmitarray, and (c) near-field focused folded transmitarray.

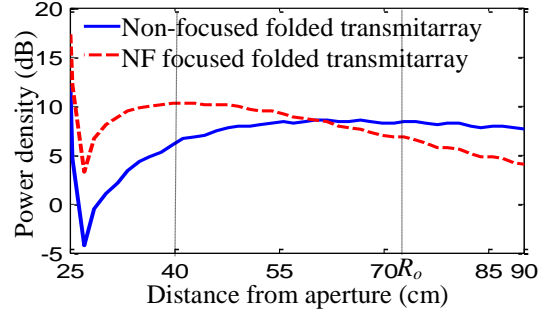


Fig. 7. The power density versus axial distance of the antenna.

IV. APPLICATION

Many people suffer from arthritis, that causes inflammation of the joints and affect anyone from young children to senior. It is typically characterized by joint pain and stiffness that make movement painful and difficult. In addition, arthritis inflammation can result from a variety of conditions and diseases, like gout, lupus and fibromyalgia. There are different arthritis heat treatment as heating pads, paraffin baths, and hot water bottles... etc. Recently, electromagnetic waves are used to treat the arthritis in an easy way. The waves are focused towards the knee to generate a localized heat. Figure 8 shows the anatomy of the part of the leg containing the knee. The electromagnetic properties of the human body at frequency 2.45 GHz are listed in Table 3 [25]. The simulation model is analyzed using the CST microwave studio with resolution $3.6 \times 3.6 \times 3.6$ mm³, to calculate its electromagnetics properties. The model with dimensions $l_w = 52$ cm and $L_h = 10$ cm containing the knee is placed at a distance $R_o = 72$ cm from the aperture of the antenna as shown in Fig. 9 (a). The contour plots of the normalized power density around the knee model in front of the transmitarray and NF-focused folded transmitarray are shown in Fig. 9 (b). The spot area is very clear in the middle of the model. The body tissues is disturbing the contour plot. The same pervious model is located at distance $R_o = 40$ cm. The contour plots at a distance of 40 cm show a more focus spot area compared with the previous state as shown in Fig. 10.

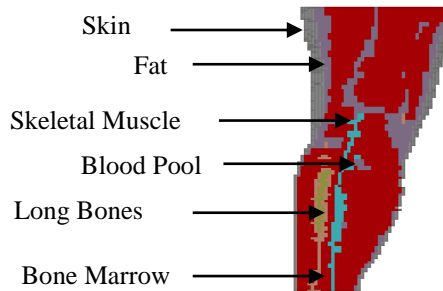


Fig. 8. The anatomy model of the part of the leg tissues [25].

Table 3: Electromagnetic properties of the human body at frequency 2.45 GHz [25]

Tissues	ϵ_r	σ (S/m)	ρ (Kg/m ³)	σ_{th} (W/K/m)
Skin	40.93	0.89	1100	0.293
Fat	5.34	0.08	1100	0.201
Skeletal muscle	55.19	1.49	1040	0.46
Long bones	12.36	0.15	1850	0.41
Bone marrow	11.19	0.23	1020	0.624
Blood pool	59.19	2.11	1000	0.505

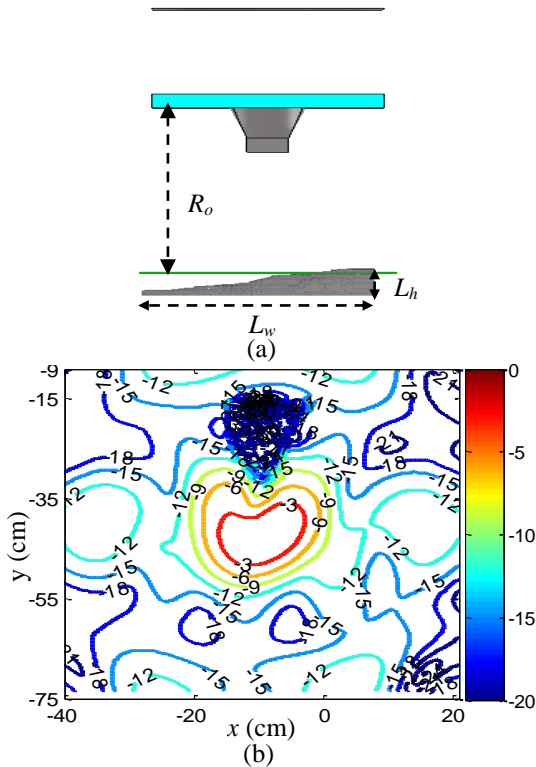


Fig. 9. (a) The construction of the antenna with the anatomy model at $R_o = 72$ cm, and (b) the contour plot of the normalized power density.

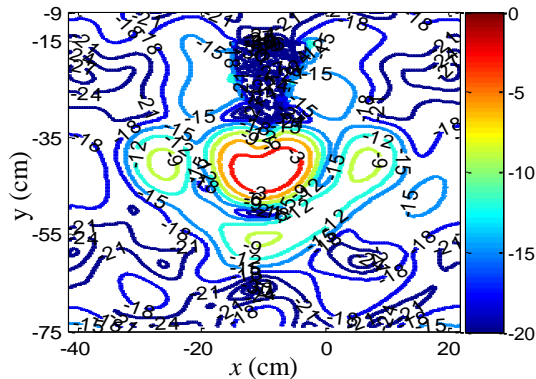


Fig. 10. The contour plot of the normalized power density at $R_o = 40$ cm.

V. CONCLUSION

A NF-focused folded transmitarray to operate at 2.45 GHz for medical applications has been investigated. The proposed antenna has a compact structure and low profile. The approach depends on focusing the radiated waves in small spot area in the near field region. The unit-cell element of the array consists of a square dielectric box with four identical circular holes. The transmission coefficient phase variation is achieved from 0 to 320 degrees while the transmission coefficient magnitude variation from 0 to -3.2 dB. The radiation characteristics of a 9×9 unfolded, folded, and NF-focused folded transmitarray are investigated. The peak gain is 21.4 dB with 1-dB bandwidth is 200 MHz for folded transmitarray. A model for the part of the human leg is used in front of the transmitarray to show the normalized power density in the near field region around it. The spot area is very clear in the middle of the model. The folded transmitarray size used in this application is 54×54 cm². Focused spot area is around 7.5×7.5 cm².

REFERENCES

- [1] O. Yurduseven and O. Yurduseven, "Compact parabolic reflector antenna design with cosecant-squared radiation pattern," *Microwaves, Radar and Remote Sensing Symposium*, Kiev, Ukraine, pp. 382-385, 2011.
- [2] G. M. Rebeiz, K. J. Koh, T. Yu, D. Kang, C. Y. Kim, Y. Atesal, B. Cetinoneri, S. Y. Kim, and D. Shin, "Highly dense microwave and millimeterwave phased array T/R modules and butler matrices using CMOS and SiGe RFICs," *IEEE International Symposium on, Phased Array Systems and Technology (ARRAY)*, Boston, Massachusetts, USA, pp. 245-249, Oct. 2010.
- [3] S. M. Gaber, *Analysis and Design of Reflectarrays/Transmitarrays Antennas*, Ph.D. Thesis, Faculty of Electronic Engineering, Menoufiya University, Menouf, Egypt, 2013.
- [4] S. H. Zainud-Deen, W. M. Hassen, H. A. Malhat, and K. H. Awadalla, "Radiation characteristics enhancement of dielectric resonator antenna using solid/discrete dielectric lens," *Advanced Electromagnetics*, vol. 4, no. 1, pp. 1-8, Feb. 2015.
- [5] J. Y. Lau, *Reconfigurable Transmitarray Antennas*, Ph.D. Thesis, University of Toronto, Canada, 2012.
- [6] J. Reis, Z. Al-Daher, N. Copner, R. Caldeirinha, and T. Fernandes, "Two-dimensional antenna beam steering using metamaterial transmitarray," *9th European Conference on Antenna and Propagation (EUCAP)*, Lisbon, Portugal, pp. 1-5, Apr. 2015.
- [7] D. Pilz and W. Menzel, "Folded reflectarray antenna," *Electron. Lett.*, pp. 832-833, Apr. 1998.
- [8] W. Menzel and D. Kessler, "A folded reflectarray antenna for 2D scanning," *IEEE German Microwave*

- Conference*, Munich, Germany, pp. 1-4, Mar. 2009.
- [9] J. A. Zornoza, R. Leberer, J. A. Encinar, and W. Menzel, "Folded multilayer microstrip reflectarray with shaped pattern," *IEEE Trans. Antennas Propag.*, vol. 54, no. 2, pp. 501-518, Feb. 2006.
- [10] W. Menzel, D. Pilz, and M. Al-Tikriti, "Millimeter-wave folded reflector antenna with high gain, low loss, and low profile," *IEEE Antennas and Propag. Mag.*, pp. 24-29, June 2002.
- [11] S. Karimkashi and A. A. Kishk, "A new Fresnel zone antenna with beam focused in the Fresnel region," *Proceedings of XXIXth General Assembly of the International Union of Radio Science*, Chicago, IL, USA, pp. 7-16, Aug. 2008.
- [12] A. Buffi, P. Nepa, and G. Manara, "Design criteria for near-field-focused planar arrays," *IEEE Antennas and Propag. Mag.*, vol. 54, no. 1, pp. 40-50, Feb. 2012.
- [13] M. Bogosanovic and A. G. Williamson, "Microstrip antenna array with a beam focused in the near-field zone for application in noncontact microwave industrial inspection," *IEEE Trans. Instrum. Meas.*, vol. 56, no. 6, pp. 2186-2195, Dec. 2007.
- [14] K. D. Stephan, J. B. Mead, D. M. Pozar, L. Wang, and J. A. Pearce, "A near field focused microstrip array for a radiometric temperature sensor," *IEEE Trans. Antennas Propag.*, vol. 55, no. 4, pp. 1199-1203, Apr. 2007.
- [15] A. Buffi, A. Serra, P. Nepa, G. Manara, and M. Luise, "Near field focused microstrip arrays for gate access control systems," *IEEE Antennas and Propag. Society International Symp., APSURSI'09*, Charleston, SC, USA, pp. 1-4, June 2009.
- [16] R. Siragusa, P. Lemaitre-Auger, and S. Tedjini, "Near field focusing circular microstrip antenna array for RFID applications," *IEEE Antennas and Propag. Society International Symp., APSURSI'09*, Charleston, SC, USA, pp. 1-4, June 2009.
- [17] R. Siragusa, P. Lemaitre-Auger, and S. Tedjini, "Tunable near-field focused circular phase-array antenna for 5.8 GHz RFID applications," *IEEE Antennas and Wireless Propag. Letters*, vol. 10, pp. 33-36, 2011.
- [18] B. Shrestha, A. Elsherbeni, and L. Ukkonen, "UHF RFID reader antenna for near-field and far-field operations," *IEEE Antenna and Wireless Propag.*, vol. 10, pp. 1274-1277, 2011.
- [19] S. H. Zainud-Deen, H. A. Malhat, and K. H. Awadalla, "8×8 near-field focused circularly polarized cylindrical DRA array for RFID applications," *The Applied Computational Electromagnetics Society ACES*, vol. 27, no. 1, pp. 42-48, 2012.
- [20] S. H. Zainud-Deen, S. M. Gaber, H. A. Malhat, and K. H. Awadalla, "Multilayer dielectric resonator antenna transmitarray for near-field and far-field fixed RFID reader," *Progress in Electromagnetics Research C, PIER C*, vol. 27, pp. 129-142, 2012.
- [21] A. Buffi, A. A. Serra, P. Nepa, H.-T. Chou, and G. Manara, "A focused planar microstrip array for 2.4 GHz RFID readers," *IEEE Trans. Antennas Propag.*, vol. 58, no. 5, pp. 1536-1544, May 2010.
- [22] F. Tofigh, J. Nourinia, M. N. Azarmanesh, and K. M. Khazaei, "Near-field focused array microstrip planar antenna for medical applications," *IEEE Antennas and Wireless Propag. Letters*, vol. 13, pp. 951-954, 2014.
- [23] Y. Adanel, M. Wongl, C. Dale', and J. Wiartl, "Near field power density characterization of radio base station antennas using spherical harmonics optimization techniques," *European Conference on Wireless Technology*, Amsterdam, Netherlands, pp. 121-124, Oct. 2004.
- [24] R. C. Hansen, "Focal region characteristics of focused array antennas," *IEEE Trans. Antennas Propag.*, vol. 33, no. 12, pp. 1328-1337, Dec. 1985.
- [25] User's manual of CST Microwave Studio Suite 2012.